J. Fluid Mech. (1983), *vol.* 136, *pp.* 277–289
Printed in Great Britain

Low-Reynolds-number flow past an elliptic cylinder

By KAZUHITO SHINTANI,
Department of Mechanical Engineering, University of Electro-Communications, Chofu, Tokyo, Japan

AKIRA UMEMURA
Department of Mechanical Engineering, Yamagata University, Yonezawa, Yamagata, Japan

AND AKIRA TAKANO
Department of Aeronautics, University of Tokyo, Bunkyo-ku, Tokyo, Japan

(Received 27 May 1982 and in revised form 26 July 1983)

The primary objective of this paper is to obtain the detailed description of the flow field near an elliptic cylinder that is placed perpendicularly in a uniform stream at low Reynolds number. Attention is paid to the shape effects due to the flattening of the cylinder and to the inertial effects of the fluid. The analysis resorts to the method of matched asymptotic expansions. The main part of the inner expansion describes the near flow field as a Stokes flow, which is characterized by the singularities arranged at the two foci of the ellipse. The first three terms $O(R)$ (R = Reynolds number) in the inner expansion are developed, and the flow aspects under the influence of the fluid inertia are investigated. The streamline patterns with one or two vortices round a finite flat plate of zero thickness, which is a special case of the elliptic cylinder, are presented.

1. Introduction

The subject of the present paper is rather classical, and analyses based on Oseen's linearized equation were given by Tomotika & Aoi (1953), Hasimoto (1953) and Imai (1954). However, the approximate equation is thought only to be valid far from the body and insufficient for the description of the near flow field. As is well known, a more complete approach to this problem may be made by using the method of matched asymptotic expansions.

The method was developed first by Kaplun (1957) and Proudman & Pearson (1957) to determine the flows past a sphere and a circular cylinder in a slow uniform stream, and it has been used in various problems concerning low-Reynolds-number flows. Bretherton (1962) gave the detailed discussion of the slow viscous motion round a cylinder in a simple shear. Chester & Breach (1969) continued the analysis of Proudman & Pearson in the case of the flow past a sphere, and Skinner (1975) did so for the case of the flow past a circular cylinder. Such works have been reviewed in the textbook by Van Dyke (1975). Recently, Bentwich & Miloh (1978) and Sano (1981) have treated the interesting problem of the unsteady flow past a sphere, and Umemura (1982) has studied the problem of the steady flow past two equal circular cylinders.

In the present paper, Umemura's method of coordinate transformation through matching procedure is applied to the analysis of the flow past an elliptic cylinder,

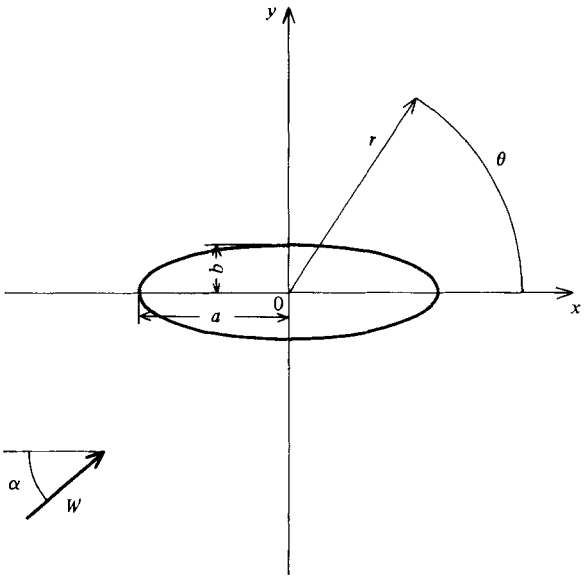

FIGURE 1. Configuration.

and the characteristics of the flow near the cylinder are discussed in detail with particular attention both to the shape effects due to the flattening of the cylinder and to the effects of fluid inertia. The shape effects can be investigated by using the elliptic coordinates for the description of the inner expansion. On the other hand, the main part of the inner expansion does not include the effects of inertia except the implicit dependence upon the Reynolds number, which results from the peculiarity of two-dimensional problems, and it describes the flow field near the cylinder as a Stokes flow.The explicit inertial effects appear first in the description of $O(R)$ for the inner expansion. The expansion procedure presented in this paper is almost along with Skinner's work for the flow past a circular cylinder except for a slight difference due to the choice of the expansion coefficients, and we shall give a simplified treatment to the matching $O(1)$, since our principal concern is the qualitative behaviour of the perturbed solutions. The first three terms $O(R)$ in the inner expansion will be developed, and the inertial effects of $O(R)$ upon the flow aspects may almost be clarified by these three terms. We shall investigate in detail the streamline patterns round a finite flat plate under the influence of fluid inertia. The familiar effect of the fluid inertia is the formation of twin vortices behind the plate. However, the asymmetric flow patterns with a single vortex also exist for the restricted range of the angle of attack.

2. Formulation

The configuration is shown in figure 1. Let us consider an elliptic cylinder placed perpendicularly in a uniform stream of velocity W. The half-lengths of the major and minor axes of the ellipse are a and b respectively. The length of the cylinder is infinite, and the flow considered is two-dimensional. The elliptic coordinates are related to Cartesian coordinates by

$$x = c\cosh\xi\cos\eta, \quad y = c\sinh\xi\sin\eta, \tag{2.1}$$

where c is the distance between the centre and the focus of the ellipse. The coordinate curves $\xi =$ constant represent a series of ellipses with the foci $(\pm c, 0)$ on the x-axis. If the surface of the elliptic cylinder is expressed by the coordinate curve $\xi = \xi_0$ then we have

$$\xi_0 = \tfrac{1}{2}\ln\frac{a+b}{a-b}, \quad \epsilon = \frac{c}{a} = \operatorname{sech}\xi_0, \tag{2.2}$$

where ϵ denotes the eccentricity of the ellipse. In addition, we take polar coordinates (r, θ), the polar axis of which coincides with the positive x-axis. The direction of the uniform stream is assumed to be at an angle α with the major axis of the ellipse. We consider the coordinates x, y and r normalized by $2a$ and the fluid velocity normalized by W, and denote dimensional quantities by the superscript * when they are needed. Corresponding with this normalization, the Reynolds number is defined by $R = 2aW/\nu$, where ν represents the kinematic viscosity of the fluid, and we assume R to be sufficiently small.

The problem is to obtain the solution of the Navier–Stokes equation

$$\nabla^4\psi = -R\cdot \mathrm{J}(\psi, \nabla^2\psi), \tag{2.3}$$

where ψ is the non-dimensional stream function normalized by $2aW$ and $\mathrm{J}(\ ,\ )$ is the Jacobian. The solution must satisfy the no-slip condition on the surface of the cylinder and approach the uniform stream at infinity.

If we seek the approximate solution of ψ valid asymptotically in the limit as $R \to 0$, the method of solution is well known. In the inner region, where $Rr \ll 1$, the governing equation for ψ is (2.3), and we assume an expansion of the form

$$\psi(\boldsymbol{r}; R) = \sum_{n=1}^{\infty} f_n(R)\,\psi_n(\boldsymbol{r}), \tag{2.4}$$

where

$$\frac{f_{n+1}(R)}{f_n(R)} \to 0 \quad \text{as} \quad R \to 0. \tag{2.5}$$

Because the flow in this region is thought to depend strongly on the body shape, we use the elliptic coordinates for the inner expansion. In the outer region, on the other hand, we introduce the outer variables $\tilde{\boldsymbol{r}} = R\boldsymbol{r}$ and $\Psi(\tilde{\boldsymbol{r}}) = R\psi(\boldsymbol{r})$, and assume an expansion

$$\Psi(\tilde{\boldsymbol{r}}; R) = \tilde{r}\sin(\theta-\alpha) + \Psi'(\tilde{\boldsymbol{r}}; R), \tag{2.6}$$

$$\Psi'(\tilde{\boldsymbol{r}}; R) = \sum_{n=1}^{\infty} F_n(R)\,\Psi_n(\tilde{\boldsymbol{r}}), \tag{2.7}$$

where

$$\frac{F_{n+1}(R)}{F_n(R)} \to 0 \quad \text{as} \quad R \to 0. \tag{2.8}$$

The first term of the right-hand side of (2.6) represents the uniform stream, and the governing equation for Ψ' becomes

$$\tilde{\nabla}^4\Psi' - \boldsymbol{e}\cdot\tilde{\nabla}\tilde{\nabla}^2\Psi' = -\mathrm{J}(\Psi', \tilde{\nabla}^2\Psi'), \tag{2.9}$$

where $\boldsymbol{e}$ is the unit vector in the direction of the uniform stream. Because the flow field far from the body is thought to be little affected by its shape and described by a function with a singularity at the origin, we use the polar coordinates for the outer expansion.

The expansion (2.4) is to satisfy the no-slip condition on the cylinder surface and the expansion (2.6) the uniform stream condition at infinity, and the construction of the solution can be completed by the matching procedure applied in the

overlapping domain of the two regions ($r \to \infty$, $\tilde{r} \to 0$). In this procedure, we use the transformation equations

$$\xi \approx \ln\left(4\frac{a}{c}\frac{\tilde{r}}{R}\right), \quad \eta \approx \theta, \tag{2.10}$$

which are correct in the approximation $O(R)$.

3. Stokes flow

If the expansions (2.4) and (2.7) are substituted into (2.3) and (2.9) respectively, we obtain a series of perturbation equations for ψ_n and Ψ_n by choosing f_n and F_n properly. As far as the order of approximation is lower than $O(R)$, we take $f_{0,n} = F_{0,n} = 1/(\ln R)^n$, and the perturbation equations for $\psi_{0,n}$ and $\Psi_{0,n}$ become the Stokes and the Oseen equations respectively, where the subscript 0 indicates the zeroth order of R.

Expressed by the elliptic coordinates, the Stokes equation becomes

$$h^2 \Delta h^2 \Delta \psi = 0, \tag{3.1}$$

where

$$\Delta = \frac{\partial^2}{\partial \xi^2} + \frac{\partial^2}{\partial \eta^2}, \quad h = \frac{2a}{c}\frac{1}{(\cosh^2\xi - \cos^2\eta)^{\frac{1}{2}}}. \tag{3.2}$$

The required solution of (3.1) to this order can easily be obtained by the method of separation of variables, and we have

$$\begin{aligned}\psi_{0,n}\Big/\frac{c}{2a} = {} & A_n\{(\xi-\xi_0)\cosh\xi + \sinh\xi_0\cosh\xi_0\cosh\xi - \cosh^2\xi_0\sinh\xi\}\cos\eta \\ & - B_n\{(\xi-\xi_0)\sinh\xi - \sinh\xi_0\cosh\xi_0\sinh\xi + \sinh^2\xi_0\cosh\xi\}\sin\eta,\end{aligned} \tag{3.3}$$

which already satisfies the no-slip condition on the cylinder surface.

On the other hand, the general solution of the Oseen equation in the polar coordinates was well investigated by Tomotika & Aoi (1950), and the required part of the solution is

$$\Psi_{0,n} = C_n \sum_{m=1}^{\infty} \phi_m(\tfrac{1}{2}\tilde{r})\,\tilde{r}\,\frac{\sin m(\theta-\alpha)}{m} + D_n \sum_{m=0}^{\infty} \chi_m(\tfrac{1}{2}\tilde{r})\,\tilde{r}\,\frac{\cos m(\theta-\alpha)}{m}, \tag{3.4}$$

where

$$\phi_m = 2K_1 I_m + K_0(I_{m-1} + I_{m+1}), \quad \chi_m = \tfrac{1}{2}\epsilon_m K_0(I_{m-1} - I_{m+1}), \tag{3.5}$$

and I_m and K_m are the modified Bessel functions of the first and second kind respectively, ϵ_m being the Neumann factor. The solution (3.4) is of course the homogeneous one for the perturbation equation (2.9). Although the particular solutions exist for $\Psi_{0,n}$ $(n \geqslant 2)$ and also participate in the matching $O(1)$, the lowest-order contribution from them to the inner expansion is $O[1/(\ln R)^3]$ and affects only the determination of the constants A_n and B_n $(n \geqslant 3)$. For simplicity we shall neglect the contributions from the particular solutions in the matching $O(1)$.

If the matching condition is applied between (3.3) and (3.4) together with the use of (2.10), we obtain the recurrence formulae for A_n, B_n, C_n and D_n, which yield the results

$$\left.\begin{aligned} &\begin{bmatrix} A_n \\ B_n \end{bmatrix} = \frac{t_+^{n-1} - t_-^{n-1}}{t_+ - t_-}\begin{bmatrix} A_2 \\ B_2 \end{bmatrix} + \frac{t_+ t_-^{n-1} - t_+^{n-1} t_-}{t_+ - t_-}\begin{bmatrix} A_1 \\ B_1 \end{bmatrix}, \quad A_1 = \sin\alpha, \quad B_1 = \cos\alpha, \\ &A_2 = \tfrac{1}{2}A_1\{2(\Gamma - p) - \cos 2\alpha\} + \tfrac{1}{2}B_1 \sin 2\alpha, \\ &B_2 = \tfrac{1}{2}A_1 \sin 2\alpha + \tfrac{1}{2}B_1\{2(\Gamma - q) + \cos 2\alpha\}, \\ &C_n = A_n \sin\alpha + B_n \cos\alpha, \quad D_n = -A_n \cos\alpha + B_n \sin\alpha, \end{aligned}\right\} \tag{3.6}$$

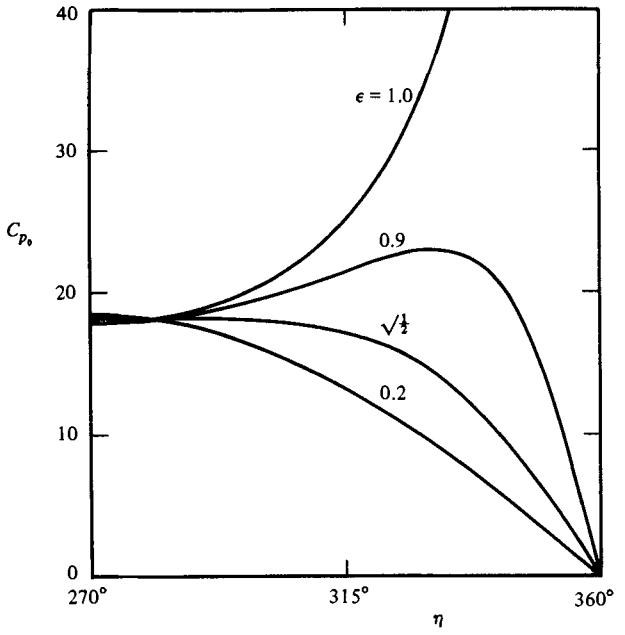

FIGURE 2. Pressure distributions on elliptic cylinders in Stokes flow for $\alpha = 90°$ and $R = 0.1$. The pressure coefficient C_{p_0} is defined by $C_{p_0} = p_0^*/\frac{1}{2}\rho W^2 = p_0/\frac{1}{2}R$, where ρ denotes the density of the fluid.

where

$$\left.\begin{aligned} t_\pm &= \tfrac{1}{2}\{2\Gamma - p - q \pm [1 + 2(p-q)\cos 2\alpha + (p-q)^2]^{\frac{1}{2}}\} \\ p &= -2\ln 2 - \ln\frac{a}{c} + \xi_0 + \tfrac{1}{2}(1 + e^{-2\xi_0}), \\ q &= -2\ln 2 - \ln\frac{a}{c} + \xi_0 + \tfrac{1}{2}(1 - e^{-2\xi_0}), \\ \Gamma &= \tfrac{1}{2} - \gamma + 2\ln 2, \end{aligned}\right\} \tag{3.7}$$

and γ is Euler's constant. We can sum up the main part of the inner expansion determined above as $\psi_0 = \Sigma_{n-1}^{\infty} \psi_{0,n}/(\ln R)^n$, which is exact to $O[1/(\ln R)^2]$ and can be obtained if we replace A_n and B_n with

$$\begin{bmatrix} A \\ B \end{bmatrix} = \sum_{n-1}^{\infty} \frac{1}{(\ln R)^n} \begin{bmatrix} A_n \\ B_n \end{bmatrix} = \frac{\begin{bmatrix} A_2 \\ B_2 \end{bmatrix} + (\ln R - t_+ - t_-)\begin{bmatrix} A_1 \\ B_1 \end{bmatrix}}{(\ln R - t_+)(\ln R - t_-)} \tag{3.8}$$

in (3.3). The flow field determined by ψ_0 is what is called the Stokes flow, the characteristics of which will be investigated below.

The pressure and the vorticity in the Stokes flow can be calculated from ψ_0 as

$$p_0 \Big/ \frac{8a}{c} = A\hat{p}_V + B\hat{p}_U, \quad \omega_0 \Big/ \frac{8a}{c} = A\hat{\omega}_V + B\hat{\omega}_U, \tag{3.9}$$

where

$$\hat{p}_V = \hat{\omega}_U = \frac{\cosh\xi \sin\eta}{\cosh 2\xi - \cos 2\eta}, \quad \hat{p}_U = -\hat{\omega}_V = \frac{\sinh\xi \cos\eta}{\cosh 2\xi - \cos 2\eta}, \tag{3.10}$$

and the subscripts U and V denote the quantities corresponding to the uniform streams in the x- and y-directions, respectively.

We show in figure 2 the pressure distributions on the surface of the elliptic cylinder

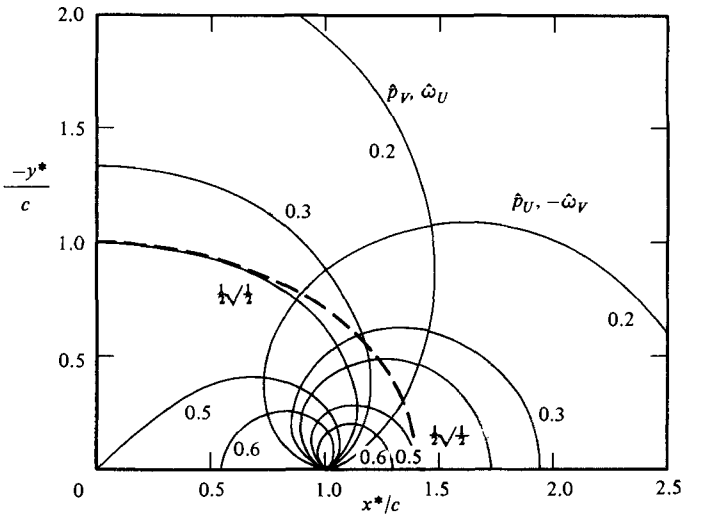

FIGURE 3. Equipressure lines and equivorticity lines in Stokes flow. The broken line represents the critical ellipse of $\epsilon = \sqrt{\frac{1}{2}}$.

when $\alpha = 90°$. We find that the aspect of the distribution for $\epsilon > \sqrt{\frac{1}{2}}$ differs from that for $\epsilon < \sqrt{\frac{1}{2}}$. When $\epsilon < \sqrt{\frac{1}{2}}$, pressure falls downstream from the stagnation point ($\eta = 270°$) nearly in the same manner as in the case of a circular cylinder. When $\epsilon > \sqrt{\frac{1}{2}}$, on the other hand, the maximum appears apart from the stagnation point. In order to see the action of the singular points, we show in figure 3 the equipressure lines and the equivorticity lines calculated from (3.10). We show only the curves in the fourth quadrant, taking the symmetry into account. Because the functions defined by (3.10) do not depend on ϵ, figure 3 shows the equipressure lines and the equivorticity lines round an elliptic cylinder of arbitrary eccentricity as a result of the normalization of the coordinate axes by c. The characteristic of the pressure distribution for $\epsilon < \sqrt{\frac{1}{2}}$ shown in figure 2 corresponds to the fact that the situation of the equipressure lines outside the critical ellipse of $\epsilon = \sqrt{\frac{1}{2}}$, which is drawn by the broken line in figure 3, is fundamentally the same as that of circular curves by a Stokeslet in the case of a circular cylinder. Namely, although the Stokes flow round an elliptic cylinder is characterized by the singularities arranged at the two foci of the ellipse, the effect of the singularities being separated from each other does not substantially reach outside the cylinder surface, where the pressure field similar to that round a circular cylinder prevails. When $\epsilon > \sqrt{\frac{1}{2}}$, on the other hand, it goes beyond the cylinder surface, as a result of which the maximum of the surface pressure appears at a different point from the stagnation point. The maximum lies at the point $\eta = \cos^{-1}[(2\epsilon^2-1)^{\frac{1}{2}}/\epsilon]$, which is the intersection of the cylinder surface and the circle of radius c in the dimensional coordinates. Especially when $\epsilon = 1$, the pressure on the flat plate varies in proportion to $[1-(2x)^2]^{-\frac{1}{2}}$, and on the whole surface, except at the ends of the plate, we find that $\partial^2\psi/\partial y^2|_{y=0} = 0$ and $\partial^2\psi/\partial y^3|_{y=0} > 0$, which in general indicate the characteristics of flows at separation points. Expanded in power series of ξ and η in the neighbourhood of the focus, the equations defining the elliptic coordinates become the equations defining the parabolic coordinates:

$$x - \frac{c}{2a} \approx \frac{c}{4a}(\xi^2-\eta^2), \quad y \approx \frac{c}{2a}\xi\eta, \tag{3.11}$$

by neglecting higher-order terms, and the stream function becomes

$$\psi_V \Big/ \frac{c}{2a} \approx \tfrac{1}{3}A(\xi-\xi_0)^2(\xi+2\xi_0). \tag{3.12}$$

Therefore the independent action of the singularities is the generation of flow round the convex surface of a parabolic body. In such a flow the streamlines are also parabolas, and the maxima of the pressure along the streamlines lie on the line $x^* = c$. In the case of the elliptic cylinder, the maximum of the surface pressure lies on a circle $r^* = c$ as a result of the interaction of the singularities arranged at the two foci of the ellipse.

The anomalous behaviour of the pressure distributions mentioned above may be understood by considering the balance of the forces acting on the rectangular fluid elements, the bases of which lie on the surface of the elliptic cylinder. The shearing force $-\tau_w$ from the cylinder surface acts on the base of a fluid element. If τ is the total amount of the shearing forces acting on the other sides of the element, the balance equation of the forces in the direction of the tangent to the surface is $\tau-\tau_w-\Delta p = 0$, where Δp denotes the pressure increase in that direction. $\tau_w \approx 0$ holds at points where the direction of the normal to the surface almost agrees with that of the uniform stream. As the cylinder becomes flatter, the region of $\tau_w \approx 0$ spreads out wider, where we have $\Delta p > 0$. Especially in the case of the flat plate, we have $\tau_w = 0$ and $\Delta p > 0$ on the whole surface of the plate except its ends.

Now, we shall give the expressions for the drag and lift coefficients of the elliptic cylinder. If each stress component derived from ψ_0 is integrated on the cylinder surface, we obtain the non-dimensional forces in the x- and y-directions $F_x = -4\pi B$ and $F_y = -4\pi A$ (the moment $M = 0$), which give the drag and lift coefficients

$$\begin{aligned} C_D &= \frac{F_x\cos\alpha + F_y\sin\alpha}{\frac{1}{2}\mathbb{R}} \\ &= -\frac{4\pi}{\mathbb{R}}\frac{2\ln\mathbb{R}+1+2\gamma-8\ln 2+2\ln[1+(1-\epsilon^2)^{\frac{1}{2}}]+\left[\dfrac{\epsilon}{1+(1-\epsilon^2)^{\frac{1}{2}}}\right]^2\cos 2\alpha}{(\ln\mathbb{R}-t_+)(\ln\mathbb{R}-t_-)}, \end{aligned} \tag{3.13}$$

$$C_L = \frac{-F_x\sin\alpha + F_y\cos\alpha}{\frac{1}{2}\mathbb{R}} = \frac{4\pi}{\mathbb{R}}\frac{\left[\dfrac{\epsilon}{1+(1-\epsilon^2)^{\frac{1}{2}}}\right]^2\sin 2\alpha}{(\ln\mathbb{R}-t_+)(\ln\mathbb{R}-t_-)}, \tag{3.14}$$

where $t_\pm$ can be written by use of ϵ and α as

$$t_\pm = -\gamma+4\ln 2-\ln[1+(1-\epsilon^2)^{\frac{1}{2}}]\pm\frac{1}{2}\left\{1+2\left[\frac{\epsilon}{1+(1-\epsilon^2)^{\frac{1}{2}}}\right]^2\cos 2\alpha+\left[\frac{\epsilon}{1+(1-\epsilon^2)^{\frac{1}{2}}}\right]^4\right\}^{\frac{1}{2}}. \tag{3.15}$$

The expressions (3.13) and (3.14) are readily shown to be identical with the results obtained from the first approximation of the Oseen equation (Hasimoto 1953; Imai 1954). For $\epsilon = 0$, (3.13) reduces to

$$C_D = \frac{8\pi}{\mathbb{R}}\frac{1}{\frac{1}{2}-\gamma+3\ln 2-\ln\mathbb{R}}, \tag{3.16}$$

which is also the result for a circular cylinder obtained by Lamb (1911) using the Oseen equation. The higher-order corrections to (3.13) and (3.14) would be obtained if the

contributions from the nonlinear term of (2.9) to the inner expansion were included in the matching procedure $O(1)$, and the inner solutions $O(R^2)$ were developed using the same method that Skinner (1975) applied to a circular cylinder. It is, however, beyond our scope. In §4 we shall derive the inner solutions $O(R)$, which give no corrections to the forces exerted on the cylinder but enable us to see the generation of vortices behind it.

4. Analysis of inertial effects

Now we examine the contributions from the higher-order terms which have been omitted in the matching procedure of §3. If we write down the asymptotic form of $\Psi_{0,n}$ $(n \geqslant 1)$ as $\tilde{r} \to 0$ in more detail and investigate its contribution to the inner expansion $(F_{0,n}\Psi_{0,n}/R)$ paying attention to the terms $O(R)$, it can be inferred that the inner solution $\psi_{1,n}$ $(n \geqslant 0)$ $O(R)$ has the functional form related to 2η and the expansion coefficient for it becomes $f_{1,n} = R/(\ln R)^n$ $(n \geqslant 0)$, that is to say, the inner expansion (2.4) has the following definite form:

$$\psi = \sum_{n=1}^{\infty} \frac{1}{(\ln R)^n}\psi_{0,n} + \sum_{n=0}^{\infty} \frac{R}{(\ln R)^n}\psi_{1,n} + O(R^2). \tag{4.1}$$

By the substitution of the expansion (4.1) into (2.3), we know that the perturbation equation for $\psi_{1,0}$ or $\psi_{1,1}$ is the Stokes equation and for $\psi_{1,n}$ $(n \geqslant 2)$ it becomes the inhomogeneous equation

$$\nabla^4\psi_{1,n} = -\sum_{i+j=n} \mathrm{J}(\psi_{0,i}, \nabla^2\psi_{0,j}). \tag{4.2}$$

The rather lengthy calculation yields

$$\begin{aligned}
\psi_{1,n}\Big/\left(\frac{c}{2a}\right)^2 &= \psi^{\mathrm{h}}_{1,n} \\
&= L_n\{\cosh 2(\xi-\xi_0)-1\}\sin 2\eta \\
&\quad + M_{n,1}\{(\xi-\xi_0-\tfrac{1}{2})(\cosh 2\xi - \cosh 2\xi_0) + (\xi-\xi_0)\sinh 2\xi_0\} \\
&\quad + M_{n,2}\{\sinh 2\xi - \sinh 2\xi_0 - 2(\xi-\xi_0)\cosh 2\xi_0\} \\
&\quad - M_{n,3}\{\cosh 2\xi - \cosh 2\xi_0 - 2(\xi-\xi_0)\sinh 2\xi_0\} \\
&\quad + [M_{n,1}\{\xi-\xi_0+\tfrac{1}{2}(\mathrm{e}^{-2\xi+2\xi_0}-1)\} \\
&\quad + M_{n,3}\{\cosh 2(\xi-\xi_0)-1\}]\cos 2\eta \quad (n=0,1),
\end{aligned} \tag{4.3}$$

$$\psi_{1,n}\Big/\left(\frac{c}{2a}\right)^2 = \psi^{\mathrm{h}}_{1,n} + \psi^{\mathrm{p}}_{1,n} \quad (n \geqslant 2), \tag{4.4}$$

where the superscripts h and p denote the homogeneous and particular solutions of (4.2), and each of them satisfies the no-slip condition on the cylinder surface.† The asymptotic forms of $\psi_{1,0}$ and $\psi_{1,1}$ as $r \to \infty$ become $r^2\sin 2(\theta-\alpha)$ and/or r^2 except the multiplication of constants. In other words, $\psi_{1,0}$ and $\psi_{1,1}$ are the solutions for the Stokes flow round an elliptic cylinder which is placed in a pure straining flow or in a rigid-body rotational flow. These perturbed solutions, which are derived from the Stokes equation, represent the effects due to the inertia of the fluid in the far flow field.

† The very long expression for $\psi^{\mathrm{p}}_{1,n}$ and the subsequent mathematical details in this section have been lodged in the editor's files, and copies of them are obtainable either from the first author or from the editorial office.

Before we determine the unknown coefficients L_n and $M_{n,1} \sim M_{n,3}$ $(n = 0, 1, 2)$ in (4.3) and (4.4) by applying the matching condition, we must know the contribution from the particular solution $\Psi^{\mathrm{p}}_{0,2}$ in $\Psi_{0,2}$, which was omitted in the matching procedure treated in §3. The perturbation equation for $\Psi_{0,2}$ was originally

$$\tilde{\nabla}^4\Psi_{0,2} - \boldsymbol{e}\cdot\tilde{\nabla}\tilde{\nabla}^2\Psi_{0,2} = -\mathfrak{J}(\Psi_{0,1}, \tilde{\nabla}^2\Psi_{0,1}), \tag{4.5}$$

and the particular solution of this equation can be written in the integral representation

$$\frac{\partial\Psi^{\mathrm{p}}_{0,2}}{\partial X} = -\frac{1}{2\pi}\int_0^{2\pi}\int_0^{\infty} \tilde{r}_1\,\mathrm{d}\tilde{r}_1\,\mathrm{d}\theta_1\{\ln|\tilde{\boldsymbol{r}}-\tilde{\boldsymbol{r}}_1| + \mathrm{e}^{\frac{1}{2}(X-X_1)}K_0(\tfrac{1}{2}|\tilde{\boldsymbol{r}}-\tilde{\boldsymbol{r}}_1|)\}F(\tilde{r}_1,\theta_1), \tag{4.6}$$

where $\tilde{r}_1$ and θ_1 are the integration variables, and we have defined $X = \tilde{r}\cos(\theta-\alpha)$, $F(\tilde{r},\theta) = -\mathfrak{J}(\Psi_{0,1}, \tilde{\nabla}^2\Psi_{0,1})$. Although it would be very hard to obtain the definite form of $\Psi^{\mathrm{p}}_{0,2}$, we can easily find its contribution to the matching $O(R)$ in the description of the inner variables by examining the corresponding part of the inner expansion for the flow round a circular cylinder. The careful examination reveals that $\Psi^{\mathrm{p}}_{0,2}$ should have the following contribution to the matching of that order:

$$\Psi^{\mathrm{p}}_{0,2} \approx \{\tfrac{1}{16}(\ln\tilde{r})^2 - \tfrac{1}{8}(\Gamma+\tfrac{1}{4})\ln\tilde{r} + C\}\tilde{r}^2\sin 2(\theta-\alpha) \tag{4.7}$$

as $\tilde{r}\to 0$. The constant C can be evaluated from (4.6), and we find $C \approx 0.0515$.

The adopted matching procedure is as follows. We first rewrite the asymptotic forms of the inner solutions (4.3) and (4.4) as $r\to\infty$ in terms of the outer variables. As for the outer solutions, we write down the asymptotic forms of (3.4) for $\Psi_{0,1}$ and $\Psi_{0,2}$ as $\tilde{r}\to 0$, of which we need only the functions related to 2θ and those of $\tilde{r}$ alone. Moreover, the asymptotic form (4.7) of $\Psi^{\mathrm{p}}_{0,2}$ must be taken into account for $\Psi_{0,2}$. And paying attention to the expansion coefficients $f_{1,n}$ and $F_{0,n}$, we have determined L_n and $M_{n,1} \sim M_{n,3}$ $(n = 0, 1, 2)$ so that both of the expansions may agree in the limit $R\to 0$.

5. Flow aspects

Let us first examine the shearing-force distributions on the surface of the elliptic cylinder. If the shear-stress component of the pressure tensor is evaluated on the cylinder surface $\xi = \xi_0$, we have

$$p_{\xi\eta}|_{\xi=\xi_0} = -h^2\left.\frac{\partial^2\psi}{\partial\xi^2}\right|_{\xi=\xi_0}. \tag{5.1}$$

The substitution of

$$\psi = \psi_0 + \sum_{n=0}^{2}\frac{R}{(\ln R)^n}\psi_{1,n} \tag{5.2}$$

into (5.1) yields $p_{\xi\eta}|_{\xi=\xi_0}$ as a function of α, ϵ and R. In the following we typically show the results for $R = 0.1$. Figure 4(*a*) shows the shearing-force distributions on the rear surface of the cylinder for $\alpha = 90°$ and several values of ϵ near unity, where the broken lines represent the results for the Stokes flow. As easily inferred from (5.1), a turning point of C_{f} corresponds to a branch point of the zero streamline. C_{f} changes its sign at $\eta = 90°$ for $\epsilon < 0.999$, and the zero streamline branches only at the rear stagnation point. For $\epsilon > 0.999$, on the other hand, C_{f} changes its sign also at the other two points, where the zero streamline separates from the cylinder surface, that is to say, the twin vortices appear. It should, however, be noted that $\epsilon = 0.999$ is not the exact critical value of eccentricity, which is slightly smaller than 0.999. The

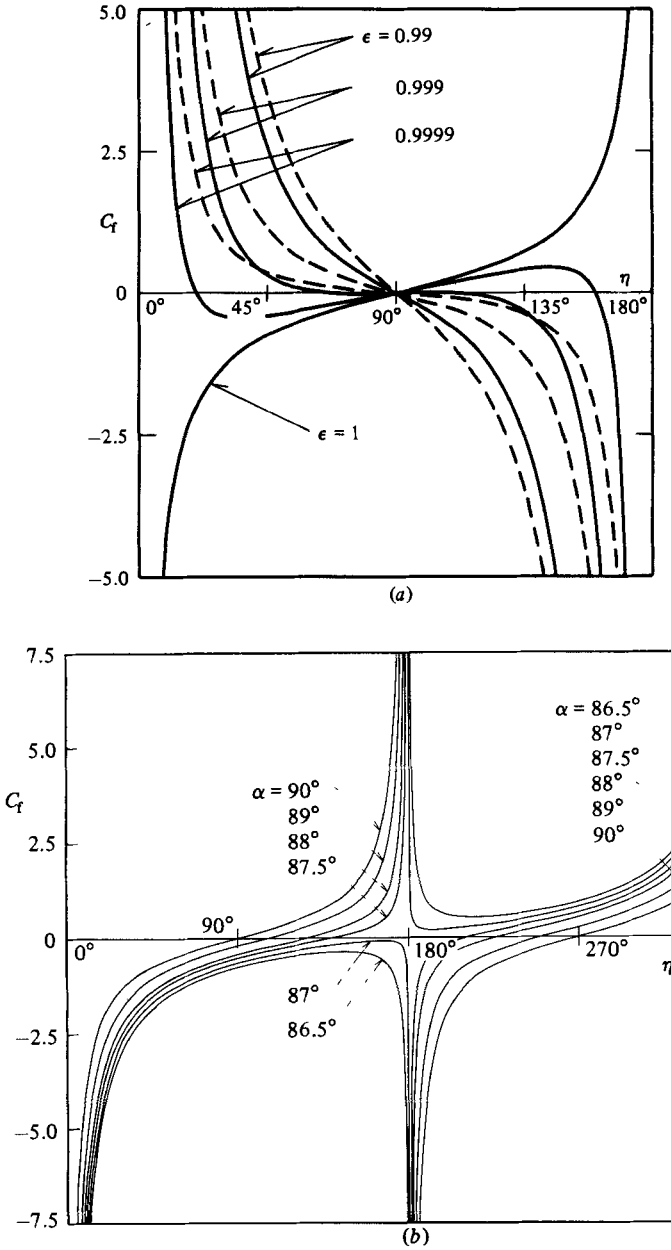

FIGURE 4. Shearing-force distributions on elliptic cylinders for $R = 0.1$. The skin-friction coefficient C_f is defined by $C_f = p^*_{\xi\eta}|_{\xi=\xi_0}/\frac{1}{2}\rho W^2 = p_{\xi\eta}|_{\xi=\xi_0}/\frac{1}{2}R$. (*a*) $\alpha = 90°$; (*b*) $\epsilon = 1$ (flat plate).

twin vortices spread out wider as the cylinder becomes flatter. Especially when $\epsilon = 1$, viz in the case of the flat plate of zero thickness, the separation occurs at each end of the plate and the standing twin vortices exist for arbitrary non-zero R if $\alpha = 90°$. It is also found from figure 4(*b*) for $\epsilon = 1$ that the zero streamline begins to separate at one end of the plate when the angle of attack α is greater than about 87°, and a single vortex is expected to be formed for the narrow range of α.

We show a series of streamline patterns round a flat plate in figure 5(*a*)–(*c*) for

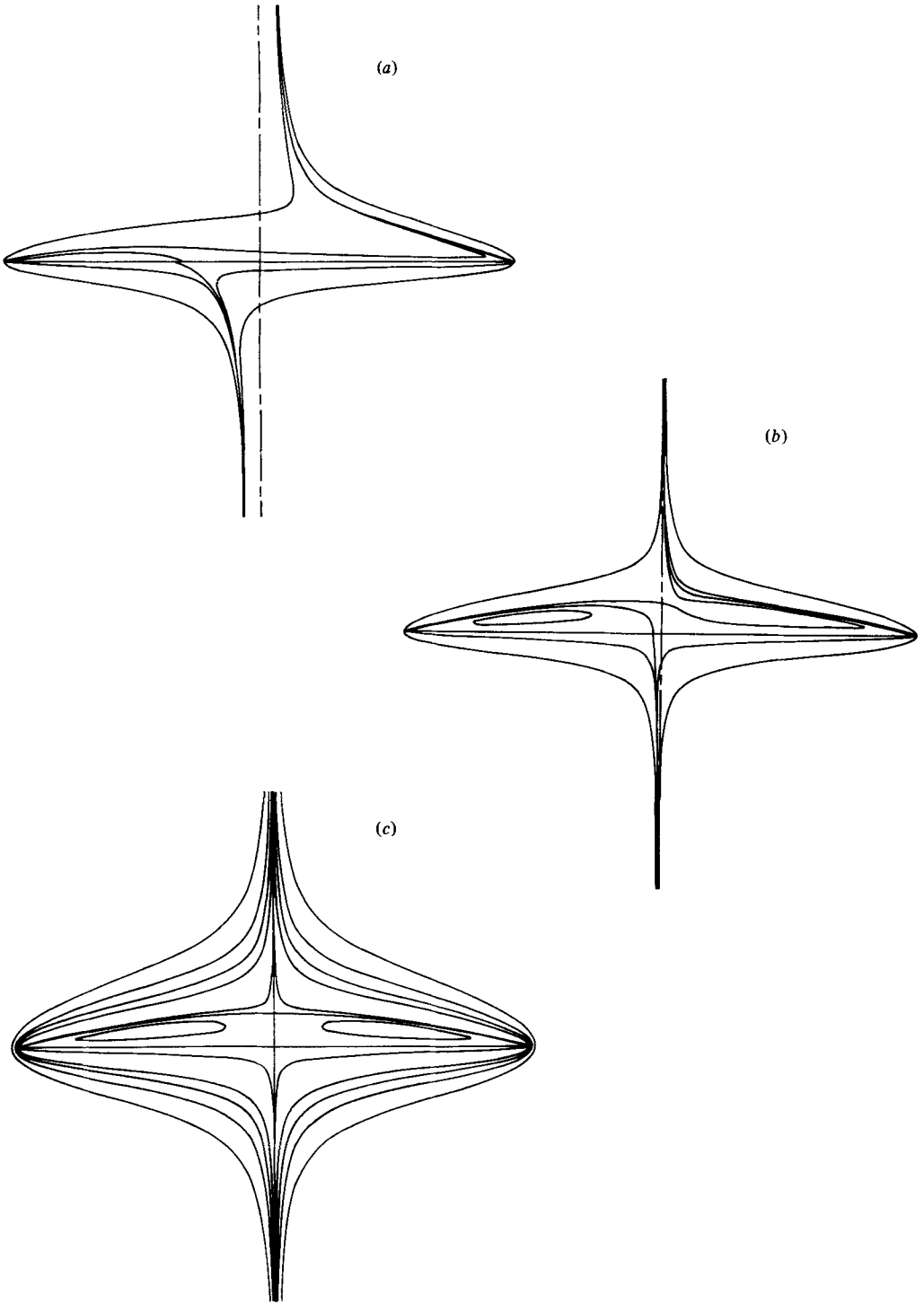

FIGURE 5. Streamline patterns round a flat plate for $R = 0.1$: (*a*) $\alpha = 89°$, $\psi = 0$, ± 0.000002, ± 0.00005; (*b*) $\alpha = 89.9°$, $\psi = -0.000002$, 0, ± 0.000002, ± 0.00005. (*c*) $\alpha = 90°$, $\psi = \mp 0.000002$, 0, ± 0.000002, ± 0.00005, ± 0.0001, ± 0.0002, ± 0.0005.

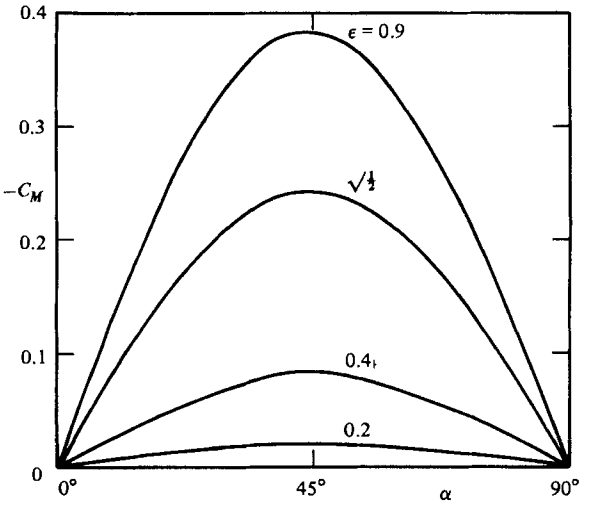

FIGURE 6. Moment coefficient for $R = 0.1$. It is defined by $C_M = M^*/\{\frac{1}{2}\rho W^2(2a)^2\} = M/\frac{1}{2}R$, where M is the non-dimensional moment around the origin.

$\alpha = 89°$, 89.9° and 90° respectively. The transition process is clearly found in these figures. A vortex region which comes out at one end of the plate grows towards the centreline as α approaches 90°. Simultaneously the branch of the zero streamline stretching from another end bends more sharply, and at last this is connected with the outer boundary line (zero streamline) of the vortex region when $\alpha = 90°$. It is also found that the constricted streamline of $\psi = 0.000002$ outside the vortex in figure 5 (*b*) is cut off to form the closed streamline inside the right-hand vortex in figure 5 (*c*). Taneda (1968) carried out a visualization of the twin vortices behind a thin flat plate of thickness ratio 0.0154 which was placed normal to the uniform stream. Figure 5 (*c*) seems to correspond with the photograph for $R = 0.440$ in his paper. The comparison should, however, be qualitative because the flat plate is of zero thickness in our calculation and its ends are singular points, so that mathematically the twin vortices, however small they may be, always appear for non-zero R. Another difficulty arises from the fact that our expansions are valid only asymptotically in the limit as $R \to 0$. The range of validity cannot be specified accurately. It can only be remarked that the calculated results for $R = 0.1$ are not so far from the exact ones to be obtained from the Navier–Stokes equation.

Finally, we can calculate from the first three terms $O(R)$ the moment exerted on the elliptic cylinder and we show it in figure 6, in which the counterclockwise moment is of positive sign, so that the head-up moment is exerted on the cylinder.

The authors are grateful to Professors Hakuro Oguchi, Koichi Oshima, Hideo Takami, Junzo Sato and Hirotoshi Kubota for many valuable comments during the course of this work. They are indebted to Professor Hidenori Hasimoto for his helpful discussion and to Professor Sadatoshi Taneda, who kindly sent one of the authors a reprint of his own paper. The authors also wish to express their thanks to the editor and the referees for many useful comments on the manuscript.

REFERENCES

BENTWICH, M. & MILOH, T. 1978 The unsteady matched Stokes–Oseen solution for the flow past a sphere. *J. Fluid Mech.* **88**, 17–32.

BRETHERTON, F. P. 1962 Slow viscous motion round a cylinder in a simple shear. *J. Fluid Mech.* **12**, 591–613.

CHESTER, W. & BREACH, D. R. 1969 On the flow past a sphere at low Reynolds number. *J. Fluid Mech.* **37**, 751–760.

HASIMOTO, H. 1953 On the flow of a viscous fluid past an inclined elliptic cylinder at small Reynolds numbers. *J. Phys. Soc. Japan* **8**, 653–661.

IMAI, I. 1954 A new method of solving Oseen's equations and its application to the flow past an inclined elliptic cylinder. *Proc. R. Soc. Lond.* A **224**, 141–160.

KAPLUN, S. 1957 Low Reynolds number flow past a circular cylinder. *J. Math. Mech.* **6**, 595–603.

LAMB, H. 1911 On the uniform motion of a sphere through a viscous fluid. *Phil. Mag.* (6) **21**, 112–121.

PROUDMAN, I. & PEARSON, J. R. A. 1957 Expansions at small Reynolds numbers for the flow past a sphere and a circular cylinder. *J. Fluid Mech.* **2**, 237–262.

SANO, T. 1981 Unsteady flow past a sphere at low Reynolds number. *J. Fluid Mech.* **112**, 433–441.

SKINNER, L. A. 1975 Generalized expansions for slow flow past a cylinder. *Q. J. Mech. Appl. Maths* **28**, 333–340.

TANEDA, S. 1968 Standing twin-vortices behind a thin flat plate normal to the flow. *Rep. Res. Inst. Appl. Mech. Kyushu Univ.* **16**, 155–163.

TOMOTIKA, S. & AOI, T. 1950 The steady flow of viscous fluid past a sphere and circular cylinder at small Reynolds number. *Q. J. Mech. Appl. Maths* **3**, 140–161.

TOMOTIKA, S. & AOI, T. 1953 The steady flow of a viscous fluid past an elliptic cylinder and a flat plate at small Reynolds numbers. *Q. J. Mech. Appl. Maths* **6**, 290–312.

UMEMURA, A. 1982 Matched-asymptotic analysis of low-Reynolds-number flow past two equal circular cylinders. *J. Fluid Mech.* **121**, 345–363.

VAN DYKE, M. 1975 *Perturbation Methods in Fluid Mechanics.* Parabolic.